



High-quality, conductive, and transparent Ga-doped ZnO films grown by atmospheric-pressure chemical-vapor deposition

Ha-Rim An^a, Hyo-Jin Ahn^{a,*}, Jeong-Woo Park^{b,**}

^aDepartment of Materials Science & Engineering, Seoul National University of Science and Technology, Seoul 139-743, Republic of Korea

^bDisplay Research Center, Samsung Display Co., Ltd., Giheung-gu, Yongin-city, Gyeonggi-do, Korea

Received 26 July 2014; accepted 3 October 2014

Available online 12 October 2014

Abstract

Ga-doped zinc oxide (GZO) thin films were prepared by atmospheric-pressure chemical-vapor deposition (APCVD) using Ga injection rates over the range 70–150 sccm. When Ga atoms substituted the Zn atoms in the ZnO matrix, the electrical resistance of GZO thin films decreased, because the dopant atom generated one extra free electron. When the injection rate of Ga was 100 sccm, a very low resistivity of $2.03 \times 10^{-4} \Omega \cdot \text{cm}$ was realized; however, the resistivity was higher when the injection rate of Ga was over 100 sccm because of the agglomeration of Ga atoms in the ZnO matrix. All GZO thin films showed an optical transmittance of over 85%; in particular, when the Ga injection rate was 100 sccm, a superior figure-of-merit (FOM) of $7.58 \times 10^{-2} \Omega^{-1}$ was found. GZO thin film prepared by APCVD could be a suitable transparent conductive oxide (TCO) material for variable optoelectronic devices.

© 2014 Elsevier Ltd and Techna Group S.r.l. All rights reserved.

Keywords: ZnO; Films; Electrical properties; Optical properties; Atmospheric pressure chemical vapor deposition

1. Introduction

Recently, transparent conductive oxide (TCO) films with low resistivity ($\rho \leq 10^{-3} \Omega \cdot \text{cm}$) and high optical transmittance ($\geq 80\%$) in the visible region (400–700 nm) have been used as electrodes for various electronic devices such as infrared reflectors, flat panel displays, and solar cells [1–3]. Well-known TCO materials are mostly n-type semiconductors (e.g., Cd-, In-, Sn-, Zn-, and Ga-based oxides) in which defects such as oxygen vacancies, interstitial metals, and dopants provide electrons to the conduction band to allow an electrical current to flow [4]. Among these TCO materials, Zn-based oxides are of special interest because of their low cost, excellent electrical properties, and distinctive optical properties [5,6]. In particular, Ga-doped ZnO (GZO) has several advantages compared to other Zn-based oxides (e.g., Al-doped ZnO

and B-doped ZnO); one is very similar atomic radius of Zn and Ga, and another is that Ga is less reactive and is resistant to oxidation [7]. These properties decrease structural deformation and increase chemical stability during doping [8].

Various techniques such as chemical-vapor deposition (CVD), sputtering, pulsed-laser deposition, and molecular-beam epitaxy have been employed to grow GZO thin films [9–12]. CVD is one of the most commonly used technologies for growing thin films because it can be used to fabricate large-area films, fast mass production, high reliability, and its ability to control the structure of films and their surface morphology [13]. Among several kinds of CVD techniques, atmospheric-pressure chemical vapor deposition (APCVD) is an attractive method because of its fast growth rate and mass production of thin films with uniform thickness [14,15]. Although the thin film deposition process is carried out at atmospheric pressure, simplifying the required equipment, there are few reports regarding GZO thin films fabricated by APCVD. Haga *et al.* prepared GZO thin films using APCVD by controlling the substrate temperature from 375 °C to 475 °C. The films were deposited with (002) preferred orientation. The best electrical properties ($\rho = 2.0 \times 10^{-3} \Omega \cdot \text{cm}$) were obtained

*Corresponding author. Tel.: +82 2 970 6622; fax: +82 2 973 6657.

**Corresponding author. Tel.: +82 31 8000 6873; fax: +82 31 8000 6822.

E-mail addresses: hjahn@seoultech.ac.kr (H.-J. Ahn),
jwjohn.park@samsung.com (J.-W. Park).

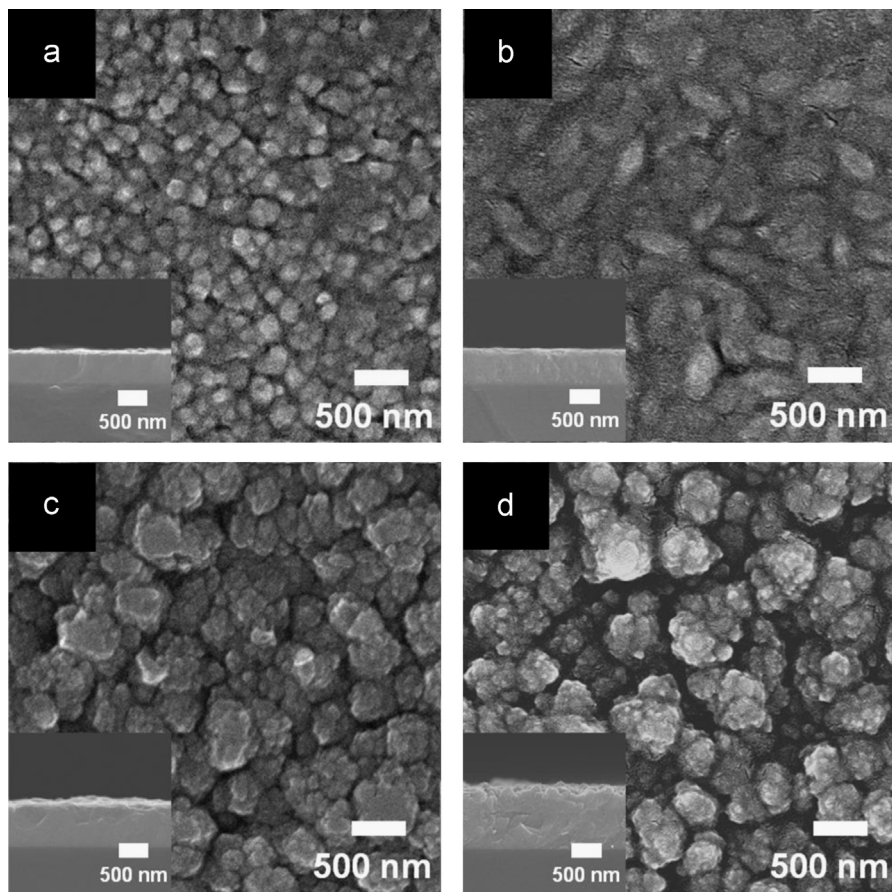


Fig. 1. Top-view and cross-sectional FESEM images of (a) sample A, (b) sample B, (c) sample C, and (d) sample D.

when GZO thin film were deposited at 425 °C [16]. In this study, we used APCVD to obtain highly conductive and transparent GZO thin films with varying concentrations of Ga. By regulating the Ga injection rate, the optimum Ga concentration in the ZnO matrix was determined, and the GZO thin films' surface morphological, compositional, electrical, and optical properties were demonstrated.

2. Experimental

2.1. Thin-film fabrication

GZO thin films were grown by APCVD on 100 × 100 mm alkali-free glass substrates. To maximize the stability of the APCVD precursors, the Zn and Ga sources were modified as ethyl groups. H₂O was used as an oxidizer to complete the Ga-doped ZnO matrix. The glass substrate temperature was maintained at approximately 550 °C, and the temperatures of Zn source, Ga source, and H₂O were fixed at 85 °C, 65 °C, and 110 °C, respectively. The injection rates of Zn source and H₂O were 3 slm and 6 slm, respectively, with N₂ carrier gas, and the injection rate of Ga source was varied over the values of 70, 100, 130, and 150 sccm, corresponding to samples A, B, C, and D, respectively. The substrates were fixed on the stage during the GZO growth process.

2.2. Thin-film characterization

The electrical properties of the GZO thin films were measured at room temperature by a Hall effect measurement system (Ecopia, HMS-3000) with van der Pauw geometry. Depth profiling of the thin films for calculating the atomic concentrations of Zn, Ga, and O was carried out by auger electron spectroscopy (AES, PHI 680). The photoluminescence (PL) properties of the GZO thin films were measured using the PL mapper (Accent, PRM2000), and the optical properties of the films were obtained with ultraviolet-visible spectroscopy (Perkin Elmer, Lambda 35) and haze meter (Murakami Color Research Laboratory, HM-150). The surface morphology and thickness of the GZO films were examined using field-emission scanning electron microscopy (FESEM; Hitachi S-4700), and their surface topology was determined using atomic force microscopy (AFM, diDimension™ 3100).

3. Results and discussion

Fig. 1 shows both the top and cross-sectional FESEM images of all the samples. The grain sizes are approximately 72–96 nm for sample A, 74–165 nm for sample B, 80–180 nm for sample C, and 96–200 nm for sample D. Figs. 1a and b show small grains grown on the films, while Figs. 1c and d show large grains. The thicknesses of samples A through D are

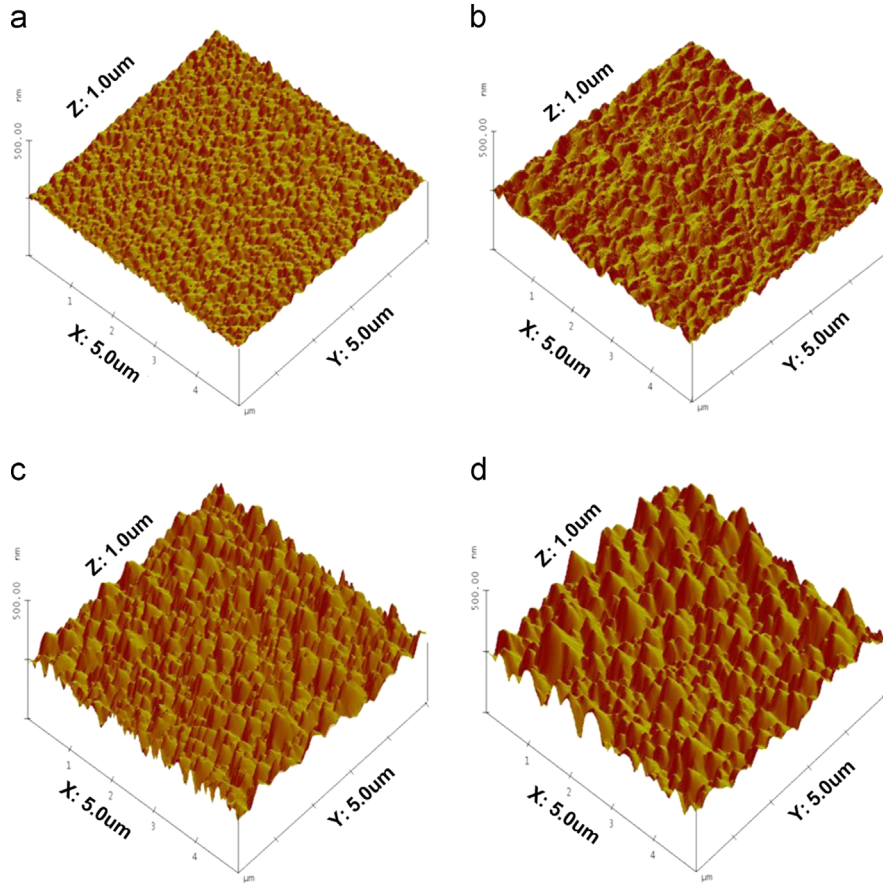


Fig. 2. Surface topologies obtained from AFM images of (a) sample A, (b) sample B, (c) sample C, and (d) sample D.

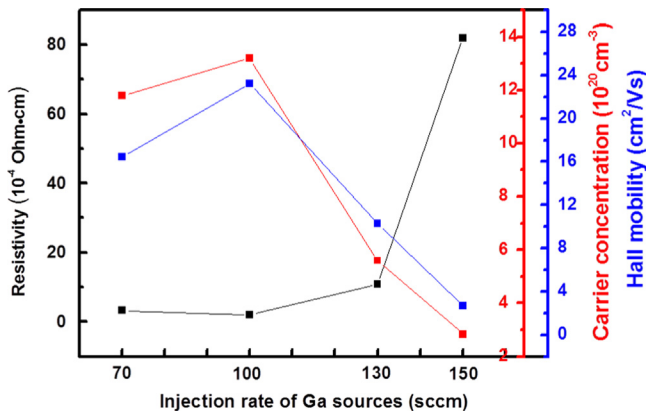


Fig. 3. Electrical properties of GZO thin films, which contain the carrier concentration, Hall mobility, resistivity, and sheet resistance with different Ga injection rate.

~510, ~550, ~690, and, ~980 nm, respectively, implying that the thicker the films, the larger the grain size because of the agglomeration and growth of small grains [17]. To further investigate the surface morphological properties of the GZO thin films, we measured the surface roughness using AFM (Fig. 2). The surface roughness values of samples A through D are 5.2, 18.0, 24.4, and, 31.0 nm, respectively. Thus, the larger the film's grain size, the higher the surface roughness.

Fig. 3 and Table 1 show the samples' electrical properties (carrier concentration, Hall mobility, resistivity, and sheet resistance). The film resistivity (ρ) depends directly on the carrier concentration and Hall mobility by the following equation [4]:

$$\rho = 1/(eN\mu)$$

where e is the electron charge (1.602×10^{-19} C), N is the carrier concentration, and μ is Hall mobility. The values of the resistivity for samples A through D are 3.22×10^{-4} , 2.03×10^{-4} , 1.08×10^{-3} , and $8.19 \times 10^{-3} \Omega \cdot \text{cm}$, respectively. The carrier concentration and Hall mobility simultaneously increased as the Ga injection rate increased up to 100 sccm, and then decreased when the injection rate was higher than 100 sccm. When the Ga concentration is lower than a certain critical value, Ga atoms substitute the Zn atoms in the ZnO matrix as dopants, producing one extra free electron per Ga dopant, resulting in very low resistivity. Therefore, the Ga concentration in the ZnO matrix may be increased as the Ga injection rate is increased. If Ga is present in excess, some Ga atoms agglomerate and not engage in the ZnO matrix, generating many defects on the GZO surface [18]. When the Ga injection rate was increased from 100 to 150 sccm, the number of free electrons decreased dramatically from $1.32 \times 10^{21} \text{ cm}^{-3}$ in sample B to $2.84 \times 10^{20} \text{ cm}^{-3}$ in sample D, and the Hall mobility also decreased from

23.22 cm²/V · s in sample B to 2.68 cm²/V · s in sample D. The sheet resistance, considering resistivity/thickness, for samples A through D is ~6.31, ~4.52, ~15.72, and ~83.65 Ω/sq, respectively. Therefore, sample B exhibited superior electrical properties owing to the highest carrier concentration and Hall mobility resulting from obtaining one electron per Ga dopant at the optimum Ga concentration.

To calculate the atomic concentration of Zn, Ga, and O as a function of different Ga injection rates, we performed AES analysis (Fig. 4). The sputter rate for the AES measurement was 5.3 nm/min for 20 min in SiO₂. The concentration of Zn, Ga, and O was almost constant, regardless of their depth in the film. Table 2 summarizes elemental analysis of all the samples. The atomic concentration of Ga in samples A through D was 2.51 %, 4.28 %, 11.16 %, and 11.73 %, respectively, indicating that the atomic concentration of Ga gradually increased on increasing the Ga injection rate.

Fig. 5 shows the PL spectra of the GZO thin films. As shown in Fig. 3, the carrier concentrations of the GZO thin films varied from 2.84 × 10²⁰ to 1.32 × 10²¹ cm⁻³, affecting the emission properties of PL spectra. The emission peaks can usually be divided into near-band-edge (NBE) emissions in the UV region because of the recombination of free excitons and broad deep-level emissions in the visible range due to defect emissions [19]. The NBE emission peaks of the GZO thin films show slight shifts toward higher energy as their carrier concentrations are increased. The NBE emission peaks of samples A, B, and C are observed at ~3.42, ~3.44, and ~3.34 eV, respectively, coinciding with the transmittance data shown in Fig. 6b, which can be explained by the Burstein–Moss effect [20]. However, the peak of sample D is difficult to be observed because the high Ga concentration suppresses PL emissions [21]. The weak emission at ~2.24 eV is due to the radiative recombination between delocalized electrons close to the conduction band and deeply trapped holes in oxygen centers [19]. The intensity of the emission peaks observed at ~2.24 eV is highest for sample D, implying that the emission properties of the GZO thin films are governed by the carrier concentrations.

Fig. 6a shows the optical transmittance of all samples. At 550 nm, the transmittances of samples A through D are ~90.52%, ~89.85%, ~86.63%, and ~85.59%, respectively. In general, the GZO thin films with higher thickness exhibit lower transmittance because of increasing optical scattering, reflection, and absorption at both the surface and in the bulk. The absorption edges of the GZO thin films between 300 and 400 nm were magnified as shown in Fig. 6b. The absorption wavelength shifts to shorter wavelengths with increasing carrier concentration in the

samples, which could be explained by the Burstein–Moss effect (the phenomenon of widening the band gap in n-type semiconductor) by using the following equation:

$$\Delta E^{\text{BM}} = h^2 / 8\pi^2 m^* \times (3\pi^2 n)^{2/3}$$

where ΔE^{BM} is the blue shift of the optical band gap, h is the Plank's constant, m^* is the electron effective mass in the conduction band, and n is the carrier concentration [22]. Therefore, the absorption wavelength of sample B, with the highest carrier concentration, shifts to the shortest wavelength. Moreover, the periodic oscillations of transmittance, presented in Fig. 6a, decrease with increasing film thickness. That is, the largest oscillation magnitude is observed for sample A, and the magnitudes gradually decrease from sample B to sample C and are hardly observed for sample D. This tendency is due to the interference between two media with different refractive indices, and becomes weak when the interface length of two media is longer than wavelength range of visible light (370–770 nm). The haze value, which defines a relationship between total transmittance and diffused transmittance, that is, haze (%) = $(T_{\text{diff}}/T_{\text{total}}) \times 100$ was measured. The average values of haze for samples A through D are ~0.6%, ~1.4%, ~3.2%, and ~8.2%, respectively; haze values increased as the transmittance decreased. Also, the haze value of the thin films is directly related to the surface roughness by the following equation [23]:

$$\text{Haze} = (4\pi \cos(\theta_i)/\lambda)^2 \times R_0 \sigma^2$$

where θ_i is the angle of incident light, λ is the wavelength of light, R_0 is the specular reflectance of the surface, and σ is the surface micro-roughness. As haze is proportional to the square of the surface roughness, sample D shows the highest value of haze. The optical properties of all the samples are summarized in Table 1.

Fig. 7 shows the FOM of all samples. The FOM evaluates the performance of films by considering optical properties and electrical properties, and is given by

$$\text{FOM} = T^{10}/R_s$$

where T is the transmittance and R_s is the sheet resistance. The FOM values for samples A through D are 5.85 × 10⁻², 7.58 × 10⁻², 1.50 × 10⁻², and 2.52 × 10⁻³ Ω⁻¹, respectively. Sample B, with the optimum Ga concentration, shows a higher FOM than other samples because of the lowest sheet resistance and high transmittance. These results show that GZO thin film fabricated by APCVD could find applications in optoelectronic devices.

Table 1
List of electrical properties containing carrier concentration, Hall mobility, resistivity, and sheet resistance and optical properties containing optical transmittance and haze values.

Samples	Carrier concentration (cm ⁻³)	Hall mobility (cm ² /Vs)	Resistivity (Ωcm)	Sheet resistance (Ω/□)	Transmittance (% , 550 nm)	Haze (%)
A	1.17 × 10 ²¹	16.44	3.22 × 10 ⁻⁴	6.31	90.52	0.6
B	1.32 × 10 ²¹	23.22	2.03 × 10 ⁻⁴	4.52	89.85	1.4
C	5.60 × 10 ²⁰	10.27	1.08 × 10 ⁻³	15.72	86.63	3.2
D	2.84 × 10 ²⁰	2.68	8.19 × 10 ⁻³	83.65	85.59	8.2

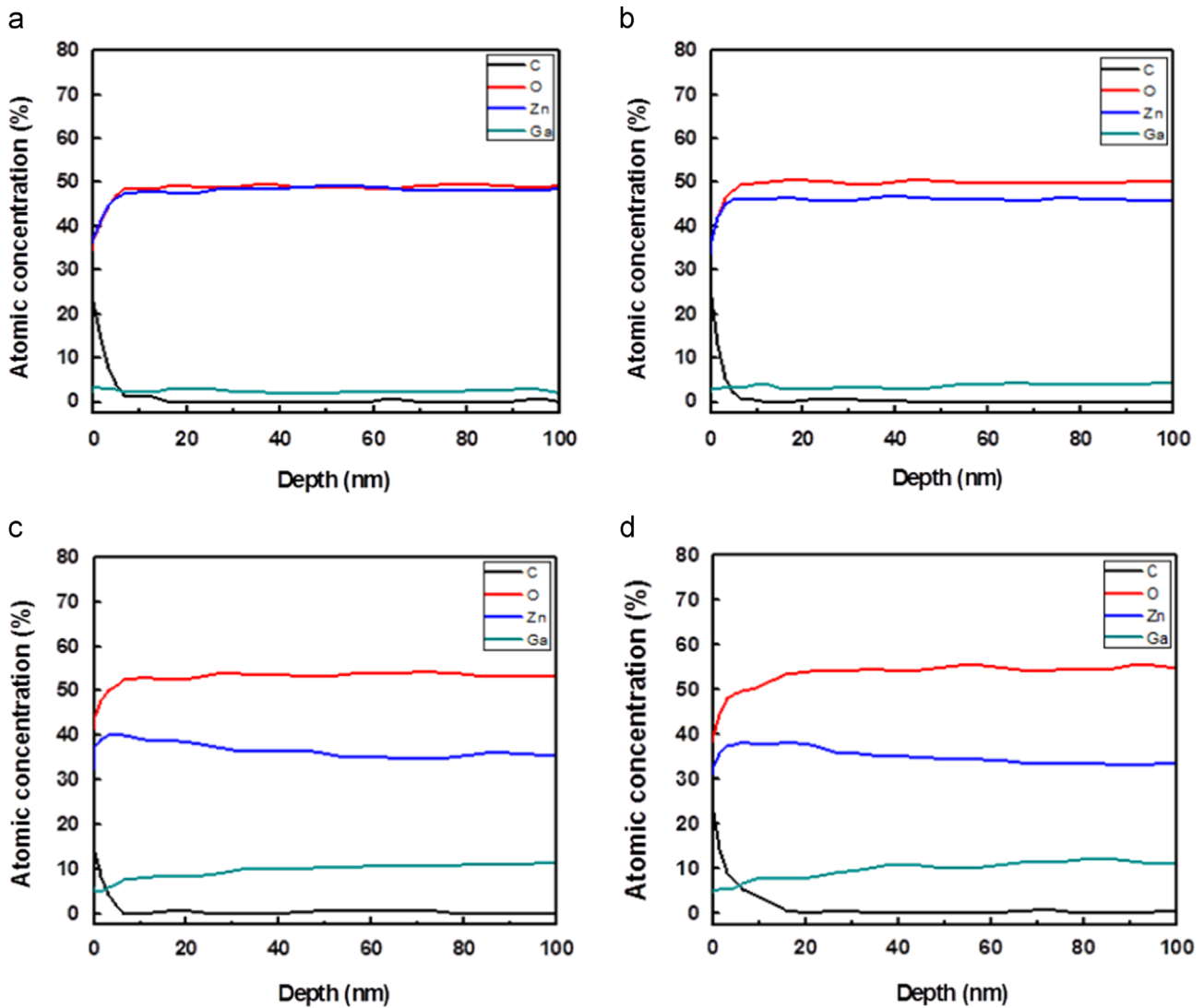


Fig. 4. Elemental analysis of (a) sample A, (b) sample B, (c) sample C, and (d) sample D grown by APCVD.

Table 2
List of contents for the Zn, Ga, and O atoms with the ratio of the atomic concentrations.

Samples	C	O	Zn	Ga
A	0	49.40	48.10	2.51
B	0	50.08	45.64	4.28
C	0	53.23	35.61	11.16
D	0	55.28	32.99	11.73

4. Conclusions

We have prepared GZO thin films using APCVD with Ga injection rates of 70, 100, 130, and 150 sccm. The compositional analysis of the resultant GZO thin films showed that the atomic concentrations of Ga in the ZnO matrix increased as the injection rates were increased. The increased injection rates improved the film electrical properties (carrier concentration and Hall mobility). However, when the injection rate was higher

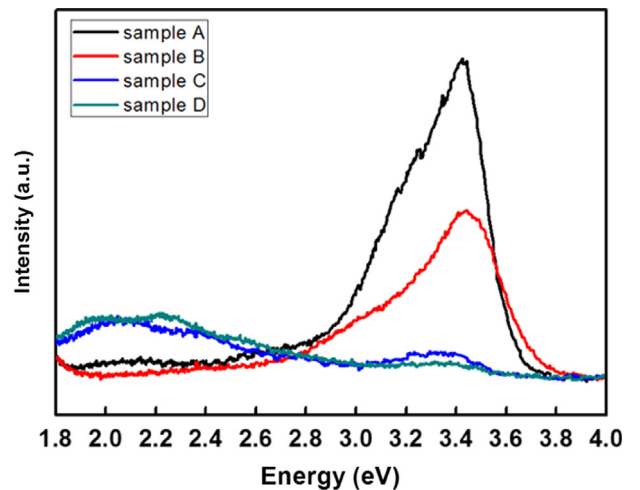


Fig. 5. PL spectra for GZO thin films with the different Ga injection rate.

than 100 sccm, the Ga concentration became very high, deteriorating the electrical properties of GZO thin films because

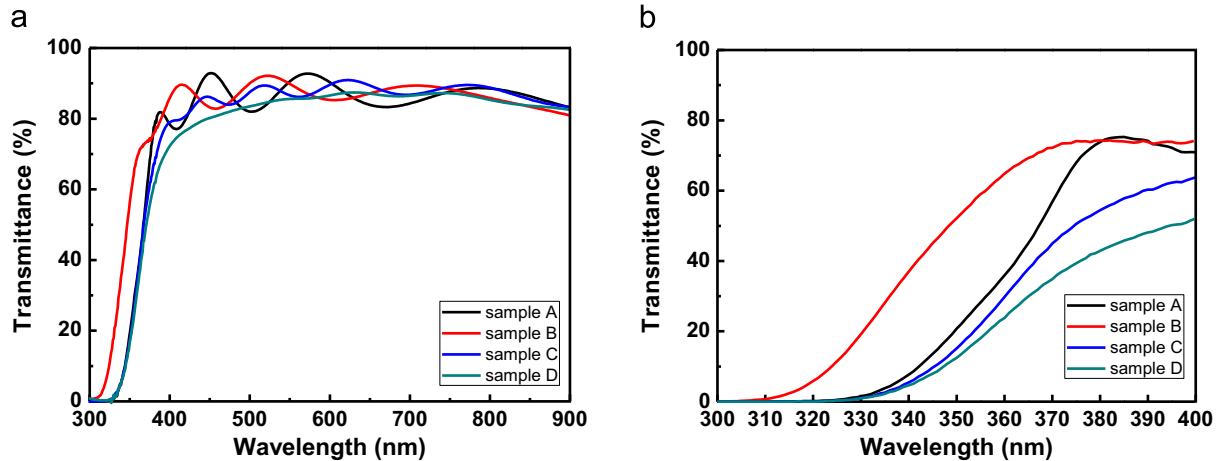


Fig. 6. (a) Optical transmittance and (b) absorption edges between 300 nm and 400 nm for GZO thin films grown by APCVD.

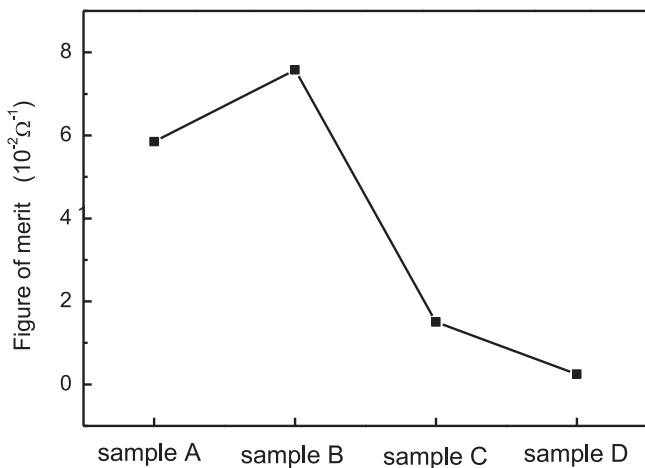


Fig. 7. Figure-of-merit (FOM) obtained from all samples.

of the agglomeration of Ga atoms. Therefore, GZO thin films prepared with the optimum Ga injection rate of 100 sccm exhibited a superior FOM ($7.58 \times 10^{-2} \Omega^{-1}$), accompanied by superb electrical resistivity ($2.03 \times 10^{-4} \Omega \cdot \text{cm}$) and good transmittance ($\sim 89.85\%$). These results could be explained by the optimum Ga concentration owing to the highest carrier concentration and Hall mobility.

Acknowledgments

This work was supported by Grant No. 10041161 from the Ministry of Knowledge Economy and the Fundamental R&D Program for Core Technology of Materials funded by the Ministry of Knowledge Economy, Republic of Korea.

References

- [1] R. Das, S. Ray, Zinc oxide—a transparent, conducting IR-reflector prepared by rf-magnetron sputtering, *J. Phys. D: Appl. Phys.* 36 (2003) 152–155.
- [2] S.K. Park, J.I. Han, W.K. Kim, M.G. Kwak, Deposition of indium-tin-oxide films on polymer on polymer substrates for application in plastic-based flat panel displays, *Thin Solid Films* 397 (2001) 49–55.
- [3] S.K. Hau, H.-L. Yip, J. Zou, A.-Y. Jen, Indium tin oxide-free semi-transparent inverted polymer solar cells using conducting polymer as both bottom and top electrodes, *Org. Electron.* 10 (2009) 1401–1407.
- [4] S. Calnan, A.N. Tiwari, High mobility transparent conducting oxides for thin film solar cells, *Thin Solid Films* 518 (2010) 1839–1849.
- [5] A.W. Ott, R.P.H. Chang, Atomic layer-controlled growth of transparent conducting ZnO on plastic substrates, *Mater. Chem. Phys.* 58 (1999) 132–138.
- [6] Q. Yang, Y. Liu, C. Pan, J. Chen, X. Wen, Z.L. Wang, Largely enhanced efficiency in ZnO nanowire/p-polymer hybridized inorganic/organic ultraviolet light-emitting diode by piezo-phototronic effect, *Nano Lett.* 13 (2013) 607–613.
- [7] X.Y. Yu, J. Ma, F. Ji, Y. Wang, X. Zhang, C. Cheng, H. Ma, Effect of sputtering power on the properties of ZnO:Ga films deposited by r.f. magnetron-sputtering at low temperature, *J. Cryst. Growth* 274 (2005) 474–479.
- [8] S.H. Lee, D.K. Cheon, W.-J. Kim, M.-H. Ham, W. Lee, Ga-doped ZnO films deposited with varying sputtering powers and substrate temperatures by pulsed DC magnetron sputtering and their property improvement potentials, *Appl. Surf. Sci.* 258 (2012) 6537–6544.
- [9] B.-T. Lee, T.-H. Kim, S.-H. Jeong, Growth and characterization of single crystalline Ga-doped ZnO films using rf magnetron sputtering, *J. Phys. D: Appl. Phys.* 39 (2006) 957–961.
- [10] J.D. Ye, S.L. Gu, S.M. Zhu, S.M. Liu, Y.D. Zheng, R. Zhang, Y. Shi, H. Q. Yu, Y.D. Ye, Gallium doping dependence of single-crystal n-type ZnO grown by metal organic chemical vapor deposition, *J. Cryst. Growth* 283 (2005) 279–285.
- [11] S.M. Park, T. Ikegami, K. Ebihara, Effects of substrate temperature on the properties of Ga-doped ZnO by pulsed laser deposition, *Thin Solid Films* 513 (2006) 90–94.
- [12] H. Kato, M. Sano, K. Miyamoto, T. Yao, Growth and characterization of Ga-doped ZnO layers on *a*-plane sapphire substrates grown by molecular beam epitaxy, *J. Cryst. Growth* 237–239 (2002) 538–543.
- [13] K.L. Choy, Chemical vapour deposition of coatings, *Prog. Mater. Sci.* 48 (2003) 57–170.
- [14] L.S. Price, I.P. Parkin, A.E. Hardy, R.H. Clark, Atmospheric pressure chemical vapor deposition of tin sulfides (SnS , Sn_2S_3 , and SnS_2) on glass, *Chem. Mater.* 11 (1999) 1792–1799.
- [15] R. Gordon, S. Barry, J. Barton, R.R. Broomhall-Dillard, Atmospheric pressure chemical vapor deposition of electrochromic tungsten oxide films, *Thin Solid Films* 392 (2001) 231–235.
- [16] K. Haga, P.S. Wijesena, H. Watanabe, Group III impurity doped ZnO films prepared by atmospheric pressure chemical-vapor deposition using zinc acetylacetonate and oxygen, *Appl. Surf. Sci.* 167–170 (2001) 504–507.
- [17] M. Sucheá, N. Katsarakis, S. Christoulakis, S. Nikolopoulou, G. Kiriakidis, Low temperature indium oxide gas sensors, *Sensor Actuat. B* 118 (2006) 135–141.

- [18] Z.-L. Lu, W.-Q. Zou, M.-X. Xu, F.-M. Zhang, Y.-W. Du, Structural and electrical properties of single crystalline Ga-doped ZnO thin films grown by molecular beam epitaxy, *Chin. Phys. Soc.* 26 (2009) 116102.
- [19] D.-T. Phan, A.A.M. Farag, F. Yakuphanoglu, G.S. Chung, Optical and photoluminescence properties of Ga doped ZnO nanostructures by sol-gel method, *J. Electroceram.* 29 (2012) 12–22.
- [20] F.K. Shan, B.I. Kim, G.X. Liu, Z.F. Liu, J.Y. Sohn, W.J. Lee, B.C. Shin, Y.S. Yu, Blueshift of near band edge emission in Mg doped ZnO thin films and aging, *J. Appl. Phys.* 95 (2004) 4772–4776.
- [21] K. Asokan, J.Y. Park, S.-W. Choi, S.S. Kim, Nanocomposite ZnO-SnO₂ nanofibers synthesized by electrospinning method, *Nanoscale Res. Lett.* 5 (2010) 747–752.
- [22] C.E. Kim, P. Moon, S. Kim, J.-M. Myoung, H.W. Jang, J. Bang, I. Yun, Effect of carrier concentration on optical bandgap shift in ZnO:Ga thin films, *Thin Solid Films* 518 (2010) 6304–6307.
- [23] V. Kanniah, E.A. Grulke, T. Druffel, The effects of surface roughness on low haze ultrathin nanocomposite films, *Thin Solid Films* 539 (2013) 170–180.